Journal of Colloid and Interface Science 504 (2017) 48–57

Contents lists available at ScienceDirect

Journal of Colloid and Interface Science

journal homepage: www.elsevier.com/locate/jcis

Regular Article

Role of Pickering stabilization and bulk gelation for the preparation and properties of solid silica foams

I. Lesov [a], S. Tcholakova [a,*], M. Kovadjieva [a], T. Saison [b], M. Lamblet [b], N. Denkov [a]

[a] Department of Chemical and Pharmaceutical Engineering, Faculty of Chemistry and Pharmacy, Sofia University, 1 J. Bouchier Ave., 1164 Sofia, Bulgaria
[b] Saint-Gobain Recherche, 39 Quai Lucien Lefranc, 93300 Aubervilliers, France

GRAPHICAL ABSTRACT

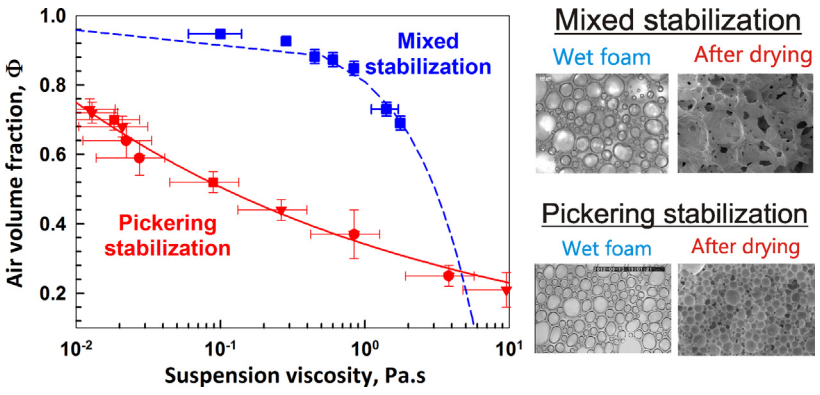

ARTICLE INFO

Article history:
Received 2 March 2017
Revised 11 May 2017
Accepted 11 May 2017
Available online 12 May 2017

Keywords:
Foams
Pickering stabilization
Ostwald ripening
Pore size
Mechanical strength
Thermal conductivity
Porous materials
Porous ceramics

ABSTRACT

Foaming of particulate suspensions, followed by foam drying, is developed as an efficient method for production of highly porous materials with various applications. A key factor for success is the appropriate choice of surfactants which both modify the particle surface and stabilize the foam. Here we compare the efficiency of this method for silica suspensions containing two surfactants which lead to very different types of foam stabilization. Cationic TTAB leads to particle-stabilized foams (Pickering stabilization) whereas zwitterionic CAPB – to surfactant-stabilized foams. Thus we determined the general (common) features shared between the various surfactant systems: (1) The foaminess is controlled exclusively by the suspension viscosity under shearing conditions which mimic precisely the foaming process; (2) The foam stability to drainage and coarsening is controlled exclusively by the suspension yield stress; (3) The surfactant adsorption on the particle surface should occur in the time scale of seconds to minutes, thus ensuring appropriate rheological properties of the foaming suspension. Similar kinetic effects could be of high interest to other colloid systems and processes, e.g. for kinetic control of the internal structure and properties of aerogels produced from sheared suspensions, and for control of the transient rheological properties and non-Newtonian flow of particulate gels.

1. Introduction

The preparation of porous materials via direct foaming has been of significant interest during the last years [1–16]. The historical overview by Binner [1] reveals that there had been several

* Corresponding author.
E-mail addresses: lesov@lcpe.uni-sofia.bg (I. Lesov), sc@lcpe.uni-sofia.bg (S. Tcholakova), mk@lcpe.uni-sofia.bg (M. Kovadjieva), tamar.saison@saint-gobain.com (T. Saison), marie.lamblet@saint-gobain.com (M. Lamblet), nd@lcpe.uni-sofia.bg (N. Denkov).

http://dx.doi.org/10.1016/j.jcis.2017.05.036
0021-9797/

attempts to develop such technique before the beginning of the new millennium. First attempts were based on the preparation of unstable surfactant-stabilized foams in the presence of particles, followed by fast polymerization of the continuous phase to avoid foam coarsening [2,3]. Later on, researchers started using proteins which enabled the preparation of more stable foams. This approach allowed better control over the porosity and morphology of the final dry materials, as well as the use of accelerated processes for consolidation of the porous structure [4], e.g. via convective drying.

In the meanwhile, more efficient procedures were developed for preparation of foams, stabilized by particles with appropriately tuned surface hydrophobicity [5,6]. This Pickering stabilization was found to provide excellent stability of the aqueous foams with respect to bubble coarsening, when particles with appropriate contact angle are used [5,6]. However, the procedures for particle hydrophobization by surface chemical treatment are usually elaborated and time-consuming, which creates difficulties in the development of robust industrial methods for preparation of porous materials by the direct foaming method.

Therefore, Gonzenbach et al. [7,8] developed a procedure for control of the particle contact angle (hydrophobicity) via *in-situ* adsorption of short-chain amphiphilic molecules with charge opposite to that of the particle surface (e.g. short-chain amines for silica at high pH). This procedure allowed the preparation of ultra-stable wet foams and dry porous materials with tunable porosity and morphology [9]. Many researchers used this approach to prepare stable wet foams or dry materials [10–16]. Some of them found that the foamability depends not only on the particle contact angle, but also on the specific surfactant used [10–13], the particle surface charge [10] and several other factors. Furthermore, the preparation of lightweight materials required not only the preparation of voluminous foams from the particulate suspensions, but also very efficient foam stabilization to coarsening, drainage [10–16] and drying [16] to avoid the foam decay upon drying. No clear relation has been established between the types of surfactant and particles used and the efficiency of this approach. For example, the assumption that short-chain surfactants with opposite charge are the best option for given particle type has not been confirmed yet as a general requirement.

In our previous study we used negatively charged silica particles in the presence of amphoteric surfactant, cocamidopropyl betaine (CAPB) which partially adsorbed on the silica surface and hydrophobized the particles [16]. In this mixed surfactant system, which contains molecules with various chain-lengths, our study showed that the longer-chain molecules adsorbed on the silica particles, whereas the shorter chain molecules remained dissolved in the aqueous phase [16]. Such CAPB-silica mixtures exhibited very good foamability which depended on suspension viscosity. On the other hand, the stability of the wet foams to drainage and coarsening was shown to depend mostly on the yield stress of the foamed suspension. After revealing the important role of suspension rheological properties for the foaming and foam stability of silica suspensions, we were able to control the foam properties and to produce dry silica materials with porosity up to 94%. However, the foams films in the respective wet foams were stabilized predominantly by surfactant adsorption layers. Therefore, upon increasing the air volume fraction above the bubble close-packing, we observed a significant bubble Ostwald ripening and formation of (partially) open-cell structure of the dry materials. The bubble Ostwald ripening was the main reason we could not obtain dry porous materials with high mechanical strength and pores with diameter below 250 μm. According to the models of Gibson and Ashby [17], porous materials with closed-cells should exhibit higher mechanical strength, while bubbles with smaller sizes are beneficial for some other properties of the dry materials, such as their thermal insulation efficiency.

Therefore, the major aims of the current study are (1) to prepare particle-stabilized (Pickering) foams from silica suspensions using a cationic surfactant TTAB, (2) to compare the foamability and the stability of the Pickering foams to the foams stabilized via suspension gelation with CAPB, (3) to prepare dry porous materials with small closed pores, low mass density, and high mechanical strength, and (4) to compare the results for the compressive strength and thermal conductivity of the materials, prepared via bulk gelation and Pickering stabilization. The obtained results clearly show that it is more difficult to obtain dry materials with required porosity when using cationic surfactant and Pickering stabilization but, when successful, this approach leads to materials with better mechanical and thermo-insulation properties in the range of low mass density of the porous materials (below ca. 150 kg/m^3).

2. Materials and methods

2.1. Materials

We used amorphous precipitated silica particles (Tixosil 365, Rhodia) with silica concentration in the batch powder ≥87.5%. The commercial powder contained additional 11.0 wt% moisture and 1.5 wt% soluble salts. According to manufacturer specifications, the specific surface area of the particles, A, is 150 ± 10 m^2/g, the mean agglomerate diameter is $d_{32} \approx 3.5$ μm, and the mass density of the silica is 2100 kg/m^3. For the modification of particle surface, we used tetradecyl trimethyl ammonium bromide (TTAB), product of Sigma with 99% purity. Deionized water from Elix 3 module (Millipore) was used for preparation of all solutions and suspensions. Analytical grade NaOH (Sigma–Aldrich) was used for adjusting the pH.

2.2. Suspension preparation

We prepared initial silica suspensions, containing 21.1 wt% silica and with pH = 8.5 using the following procedure:

97 g Tixosil was weighted in a polyethylene jar and 291 g deionized water was added. The suspension was homogenized for 2 h with a pulse sonicator (SKL-650W, Syclon), equipped with a 3 mm in diameter sonotrode, set at power output of 450 W and pulses of 1 s, separated by 0.5 s off-periods. Next, the suspension pH was adjusted to 8.5 to increase the surface charge of the silica particles. At this pH the particles had maximum surface charge, without starting to dissolve [18]. For this purpose, we added 11.94 g of 2 M NaOH solution and further homogenized the suspension with ultrasound for 60 min. Surfactant was added just before foaming to reduce the effect of the (gradual) suspension gelling on foaming, see Section 3.4. More diluted suspensions, down to 14 wt% silica, were prepared by dilution of the initial silica suspension with water before addition of the TTAB solution.

Surfactant-to-particle ratio in the studied suspensions was expressed in terms of particle surface coverage by TTAB molecules:

$$\theta = \frac{100\, C_S}{C_P A \Gamma_{max}} \ [\%] \qquad (1)$$

where $A \approx 150$ m^2/g is the specific surface area of the particles, C_S is the surfactant concentration in the suspension in wt.%, and C_P is the particle concentration in the suspension in wt% [18]. Maximum adsorption, $\Gamma_{max} \approx 1.7 \pm 0.1$ mg/m^2, was determined for TTAB dense monolayers on silica surface at pH 8.5 [18]. As shown in Section S1 in ESI, around 98% of the added TTAB is adsorbed on the particle surface in the suspensions, unless very high TTAB concentrations are used (ca. several wt% which corresponds to $\theta > 50\%$). Therefore, we use below θ as a convenient measure of the TTAB concentration,

expressed as the maximum possible (and very close to the real one) surface coverage of the silica particles by the available surfactant.

2.3. Foam generation, foam stability and preparation of porous materials

A total of 400 g suspension + TTAB solution were premixed for 2 min in a planetary mixer, model Chef Premier KMC 560, 1000 W (Kenwood), at a minimum speed (i.e. level 1 at the switch for speed control of the mixer). The suspension was then foamed for 10 min at third or seventh speed level of the mixer and the foam volume was recorded with time. Afterwards, the air volume fraction was determined independently via gravimetric measurement.

To prepare dry porous materials, we placed 114 mL of the produced wet foam in cylindrical Teflon molds (diameter 8.5 cm and height 2 cm) and monitored for several days the foam stability upon storage and drying at ambient temperature, 28 ± 5 °C, and humidity 30–45%.

Foam films and bubble Ostwald ripening were observed within 4 h, at the top of the wet foam, in reflected light, using optical microscope, Axioplan (Zeiss, Germany), equipped with long-distance objectives Zeiss Epiplan 50×/0.40 and EC Plan-Neofluar 2.5×/0.075.

The mean pore size in the final dry porous material was determined by Scanning Electron Microscopy (SEM). A small piece, ca. 5 mm in size, was taken from the middle of the sample and coated with Au/Pd alloy via low-vacuum sputter coating and imaged on SEM instrument TESCAN LYRA3 GM (Czech Republic).

2.4. Suspension rheology

The rheological properties of the suspensions were characterized by Gemini rotational rheometer (Malvern Instuments, UK) at 25 °C. We used parallel plates geometry with 20 mm radius and 500 μm gap. The plates were covered with sandpaper (P 1500, app. 12 μm grain size) to avoid wall-slip.

To mimic the suspension properties during foaming, we measured the viscosity in the following way: 25 g silica suspension in water was sonicated for 5 min at 400 W, cooled down to room temperature and TTAB was added. The suspension was stirred for 30 s with the surfactant and immediately afterwards placed in the rheometer. Viscosity was recorded as a function of time for a period of 2000 s (at different shear rates, applied to separate samples).

2.5. Mechanical strength

Tests for the mechanical properties of the dry porous materials were performed via Universal testing machine Tira GmbH Tiratest 2300, according to standard ISO 844:2009. The stress was measured with accuracy of ±1%, as a function of sample deformation (rates varied between 0.5 and 5 mm/min). The solid samples had size between 50 and 70 mm in diameter and around 1.5–2.0 cm in height. The crushing stress of these materials was determined either from the brittle crushing plateau of the stress-strain curves (see ESI Fig. S2) or from the maximum in the stress below 10% deformation (brittle failure). All measurements were performed at ambient conditions: 20 °C and 45 ± 10% rel. humidity.

2.6. Thermal conductivity

The heat conductivity of the dry porous materials was measured with HFM 436 series flowmeter (Netzsch™) according to standards ASTM C518 and ISO 8301 (the flowmeter was set at 10 °C, the air pressure was 1 bar, and ΔT was 20 K). The precision of the measurements was estimated to be ±5%.

3. Experimental results

In Sections 3.1–3.3 we present results about the preparation of the wet foams and their stability. In Section 3.4 we discuss the effect of suspension viscosity on the suspension foamability. In Sections 3.5 and 3.6 we illustrate the effect of the stabilizing mechanism of the wet foam on the mechanical and thermal properties of the final dry porous materials.

3.1. Effect of TTAB surface coverage on the foaminess of 15.7 wt% silica suspensions

The kinetics of air entrapment (foam formation) was studied first with 15.7 wt% silica suspensions, at different TTAB concentrations in the suspension. The concentration was varied in a range which would ensure TTAB coverage of the silica particles between 0.2 and 13.5%, corresponding to the range from 4 to 230 $\mu g/m^2$, upon the assumption that all surfactant molecules in the suspension are adsorbed on the particle surface. Two speeds of the planetary mixer were applied during the foaming stage in these experiments: 45 s^{-1} and 100 s^{-1}. The speeds were estimated using the model of Chesterton at al. [19].

The experimental results presented in Fig. 1A and B show that no foam was formed while stirring a silica suspension without TTAB. The original silica particles were too hydrophilic and could not stabilize the trapped air bubbles.

In the presence of TTAB, the process of air entrapment included two well defined regions: In the first region, the quantity of trapped air rapidly increased up to a given volume which remained constant upon the subsequent shearing of the system (second plateau region). To characterize the rate of air entrapment during the first region, we calculated the increase of the air volume fraction with time, $d\Phi/dt$, in the initial period in which Φ increases linearly. The respective data are plotted in Fig. 1C, as determined for both shear rates of the planetary mixer studied, 45 s^{-1} and 100 s^{-1} (cf. with Fig. 1A and B). To characterize the plateau region, we plot the final air volume fraction, as a function of θ, Fig. 1D. Both the rate of air entrapment, $d\Phi/dt$, and the air volume fraction in the plateau region, Φ_{PL}, pass through a maximum, as a function of TTAB coverage, θ. The peak was observed at $\theta \approx 1.6\%$ (viz. at very low surface coverage) for both shear rates. Both Φ_{PL} and $d\Phi/dt$ increased with the mixing rate, as expected.

Data showed also that very low TTAB coverage of the particles, e.g. $\theta = 0.6\%$, caused a significant increase of Φ_{PL} from zero (no TTAB) to $\Phi = 0.60$ at 100 s^{-1}. Data from Petit et al. [20] showed that the contact angle of silica particles should be around 30–35° at such low surface coverage, which seems to be sufficient to ensure particle adsorption on the bubbles surface and to prevent bubble coalescence during shear (see Section 3.3 for further explanations). The increase of θ from 1.6 to 6.8% reduces the volume of trapped air at both shear rates, which is explained with the increased suspension viscosity, as shown in Section 3.4.

3.2. Effect of particle concentration on the foam formation and stability

In this section we summarize the main results from the systematic experiments, aimed to clarify the effects of particle and TTAB concentrations on the foam formation and foam stability. As shown in Section 3.1, the original silica particles are too hydrophilic to stabilize the bubbles. Once TTAB is added to ensure a surface coverage

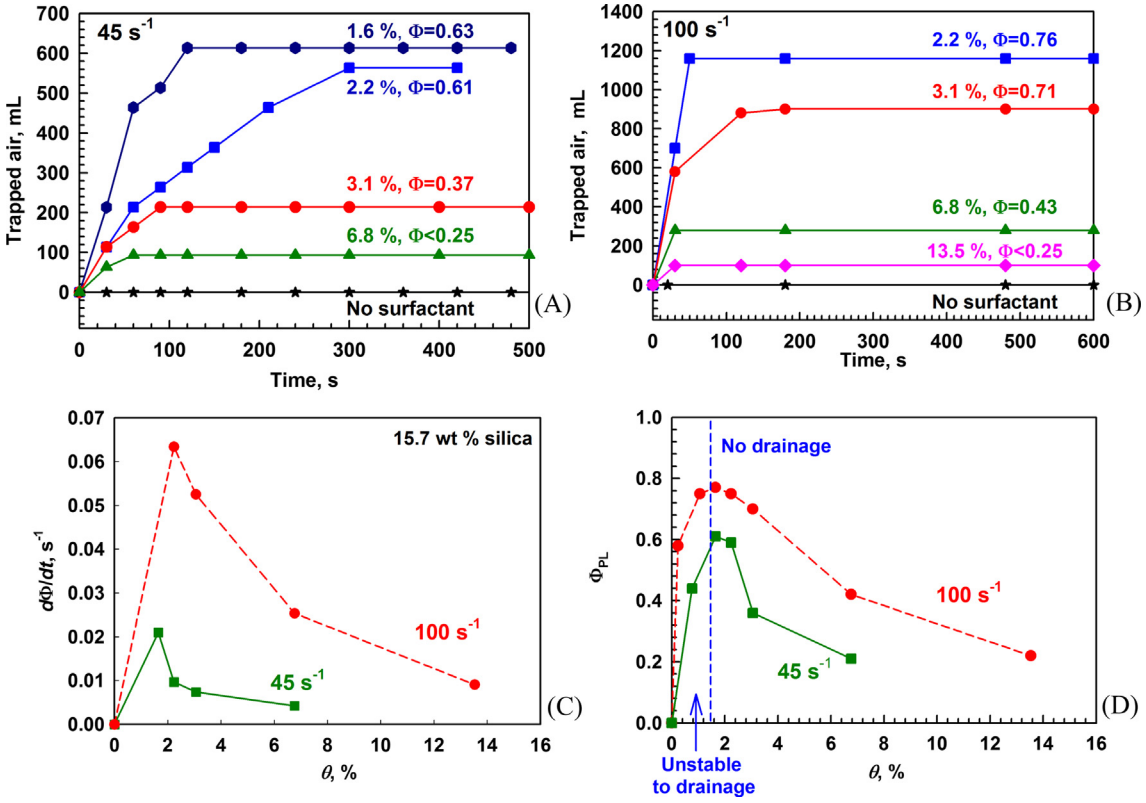

Fig. 1. Kinetics of air entrapment in a planetary mixer for suspensions containing 15.7 wt% silica particles and surfactant corresponding to TTAB coverage of the silica particles, θ [%], as indicated in the figures. Experiments were performed at (A) 45 s^{-1} and (B) 100 s^{-1}. (C) Rate of air volume fraction increase, $d\Phi/dt$, and (D) Air volume fraction in the plateau region, Φ_{PL}, as a function of θ, at 45 s^{-1} (green squares) and 100 s^{-1} (red circles). Blue vertical dashed line in (D) shows the minimum TTAB coverage for formation of stable wet foams which can be dried to produce stable porous materials. (For interpretation of the references to color in this figure legend, the reader is referred to the web version of this article.)

of θ > 0.2%, we observed two different regions with respect to suspension foamability and foam stability (Fig. 2A):

Region 1 spanned from θ = 0.2% to 6.8% for C_p = 15.7 wt%, and between 0.3 and 2.4% for C_p = 20 wt%. In this region, the suspension foamability was reasonably good and the bubble volume fraction, Φ_{PL}, in the foams formed after long foaming time was between 0.35 and 0.85. This region is of primary interest to our study, as the formed foam precursor could be dried to produce a dry porous material.

Region 2 was a vast region, observed between 3% and 71% TTAB coverage, at $C_P \approx 20$ wt%. Suspensions with composition in this region have very high viscosity and negligible foamability,

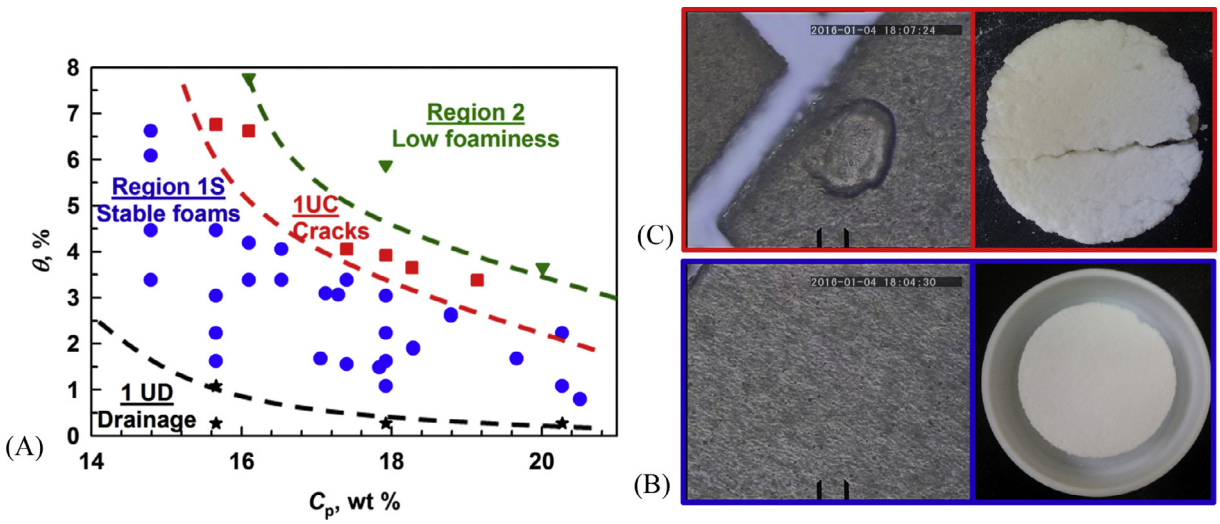

Fig. 2. (A) Foaming and stability diagram, depending on TTAB coverage of the silica, θ, and the particle concentration, Cp. Reasonably good foamability ($0.35 < \Phi_{PL} < 0.85$) was observed in Region 1 and decreased foamability in Region 2 ($\Phi_{PL} < 0.35$). (B-C) Dried wetting films and the respective porous materials, prepared from suspensions containing 15.7 wt% silica at (B) 2.2% TTAB coverage or (C) 6.8% TTAB coverage. Color coding shows the regions of foaming and stability in (A). Scale is 20 μm in (B) and (C).

Φ_{PL} < 35%. Significant particle aggregation occurred in these suspensions, observed even with naked eye.

With respect to foam stability to liquid drainage, Ostwald ripening and drying, we found that Region 1 was divided into 3 sub-regions: 1UD: Foams, which are unstable to drainage; 1S – Foams, which are stable to drainage, Ostwald ripening and drying; 1UC – foams, which were stable to drainage and ripening, but cracked upon drying. More detailed description of these sub-regions follow:

Region 1UD. This region appeared between θ = 0.2% and 1.6% TTAB at 15.7 wt% silica particles, and between 0.3% and 1.0% at 20.3 wt% silica. All foams in this region had Φ_{PL} > 0.55. During storage, the liquid phase partially drained from the foams and the air in the remaining foam increased up to 85 ± 5 vol%. After the initial water drainage, these foams seemed stable to further coarsening. However, these foams were inappropriate for preparation of porous materials, because they tended to crack upon drying, due to the inhomogeneous water distribution in the drying sample.

Region 1S. This region appeared between 1.6% and 4.7% TTAB coverage at 15.7 wt% silica, and between 1.0% and 2.2% at 20.3 wt % silica in the suspension. Φ_{PL} was between 60 and 83 vol%, depending on the surfactant and particle concentrations in the suspension. At θ ≈ 1.8%, Φ_{PL} decreased from 77% to 68%, as C_P increased from 15.8 to 20.3 wt%. Similar decrease of Φ_{PL} with the increase of C_P was observed at θ ≈ 3.5%. Generally, the increase of surfactant and/or particle concentration led to a decrease of Φ_{PL} in this region. The dry materials from Region 1S contained no visible cracks. This region allowed us to prepare very lightweight materials with porosity up to 96.2% or 80 kg/m^3 density (from 14 wt% silica suspensions with very low viscosity). Illustrative porous material, obtained in this region is shown in Fig. 3A and in the SEM micrograph in Fig. 3B. The pore diameter was typically smaller than 200 μm in these samples and the cells had closed structure.

Region 1UC. Here the suspension foamability decreased steeply and Φ_{PL} decreased down to 0.35 - see the red squares in Fig. 2A. The foams formed in this region were stable to liquid drainage and bubble coarsening, but unstable upon drying. The high presence of large particle agglomerates, like those shown in Fig. 2C, caused the formation of cracks in the drying materials, due to inhomogeneous distribution of water and of the respective capillary stresses during drying [21].

Although not shown here, we observed a region with much higher foamability at θ > 75%, see Fig. S4 in ESI. The foams in this region were stabilized by surfactant adsorption layers and suffered from severe bubble Ostwald ripening. No stable porous materials could be obtained from these foams.

3.3. Mechanisms of stabilization of the wet foams in the presence of TTAB and CAPB

As discussed above and studied in more detail in Ref. [16], the original silica particles are too hydrophilic and do not adsorb on the surface of the foam films. Illustrative image of the foam film, prepared from suspension of silica particles without any surfactant added, is presented in Fig. 4A, just before the film ruptures (these foam films were formed and observed in a capillary cell [22]). This film has a thickness of ≈30 nm, i.e. smaller than the size of the silica particles. Therefore, the film contains no particles at this stage of its thinning. Without being stabilized by particles or surfactant, this film ruptured within several seconds after it was captured in the image shown in Fig. 4A.

Upon addition of TTAB to θ = 1.1%, the contact angle of the silica particles increases [20] and they adsorb on the bubble surface, as illustrated both experimentally and schematically in Fig. 4B. This particle (Pickering) stabilization prevented the bubble coalescence and completely arrested the bubble Ostwald ripening (e.g. Fig. 5A). However, under these conditions the suspension drainage from the foam was not eliminated. To prevent drainage, we needed to induce stronger attraction between the silica particles, as schematically drawn in Fig. 4C, to provide a sufficiently high yield stress of the suspension. Indeed, upon increase of TTAB coverage to θ = 1.6% (for 15.7 wt% silica), the suspensions acquired a yield stress and behaved as a Bingham fluid (see ESI for more detailed explanations). Experimentally, we measured a yield stress of ≈4 Pa to be the threshold value preventing drainage for 250–300 μm bubbles, as observed in these systems, Fig. 4. This value is in excellent agreement with our results for CAPB-silica suspensions, where we explained that the yield stress required to prevent drainage is $\tau_{YD} \sim \Delta\rho g d$ [16,23 and ESI], where $\Delta\rho$ is the mass density difference between bubbles and the suspension, g is gravity acceleration, and d is the bubble diameter.

Thus we see that the foams are stabilized to drainage by the same mechanism, suspension gelling until the yield stress becomes $\tau_{YD} \sim \Delta\rho g d$, for both types of suspension: silica + CAPB and silica + TTAB.

The Ostwald ripening in silica + TTAB foams was completely arrested (Fig. 5A) whenever particles adsorbed on the interface (Fig. 4B-C). This result is explained by the combination of two com-

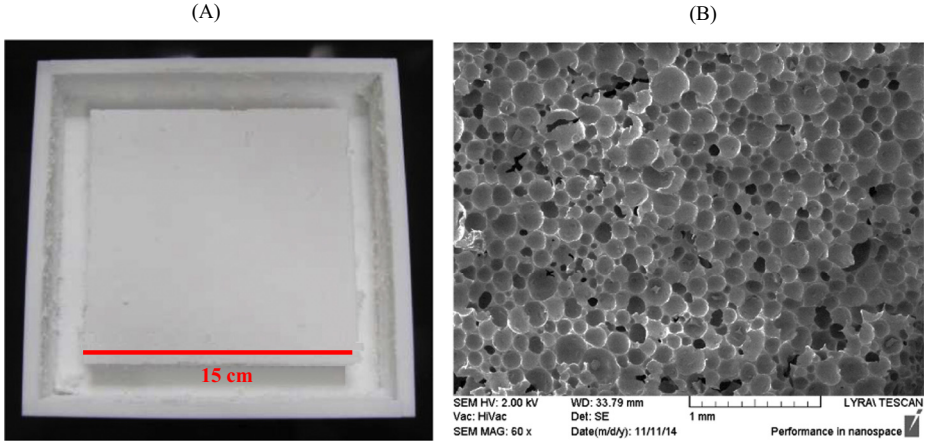

Fig. 3. (A) Illustrative images of porous material with ρ = 120 kg/m^3, prepared from a suspension with compositions falling in Region 1S, 15.7 wt% particles and 2.2% TTAB surface coverage. (B) SEM micrograph of the material in (A).

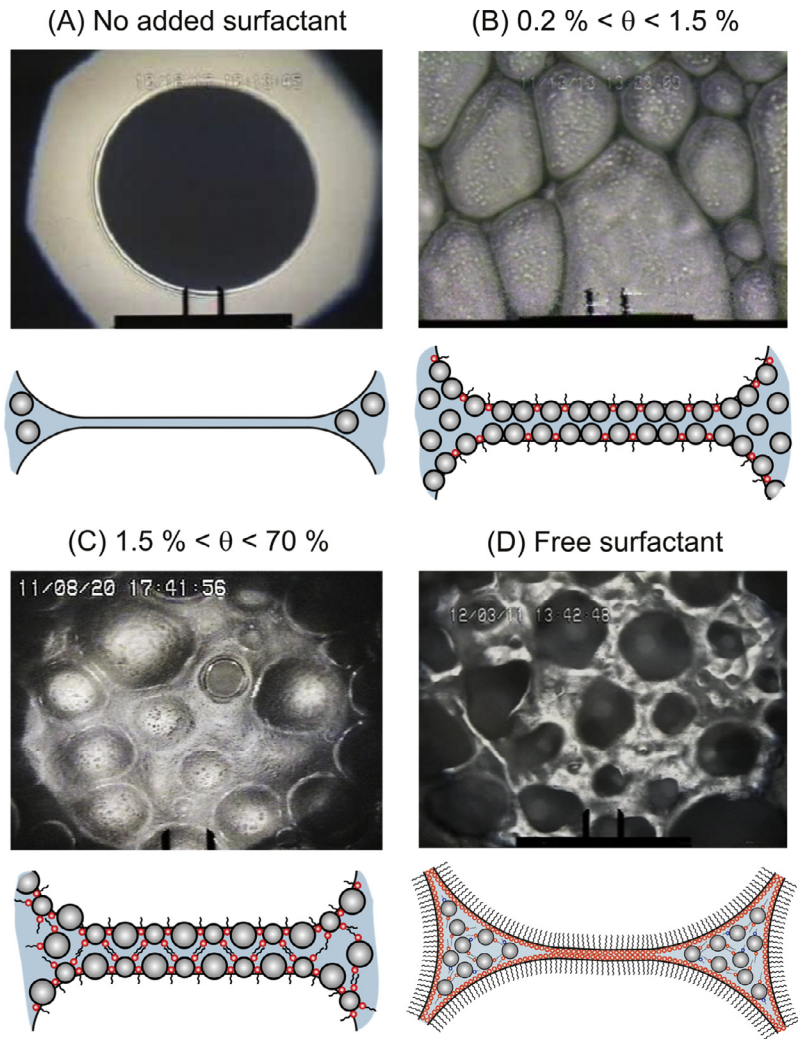

Fig. 4. Microscopic images of foams/foam films, including their schematic presentations. (A) Hydrophilic silica particles form unstable foam films; (B) Region 1U – films stabilized by TTAB-modified particles. Insufficient yield stress and large size of the bubbles cause liquid drainage from the foam; (C) Region 1S – TTAB-modified particles adsorb on the surface of the foam film and form weakly aggregated particle network in the bulk suspension; (D) Films stabilized by surfactant (no particles inside the foam films) in the presence of TTAB of large excess, while the particles form a gel in the nodes and in the Plateau channels of the foam. The foam films appear as black areas, because they reflect and scatter very little light, as compared to the particles. Scales: (A) 100 μm and (B-D) 50 μm.

plementary mechanisms. First, the particle-stabilized foam films are much thicker and, hence, the gas transfer across them is much slower, as the rate of gas transfer is proportional to the inverse of the film thickness [24]. Second, the particles are able to assemble in a jammed armoring coat on the bubble surface, thus creating a mechanical resistance to the bubble surface shrinkage (and possibly expansion) [25–27]. In addition, the gradual gelling of the bulk suspension further reinforces mechanically the obtained complex three-phase structure (air-silica-water) which can be afterwards dried to obtain final porous material of high quality [16].

In contrast, in silica + CAPB foams (Fig. 5B) we always observed relatively fast Ostwald ripening of the bubbles during the first several minutes, up to 1 h. The bubble coarsening rates in CAPB + silica foams were comparable to those of surfactant-stabilized foams [24] which is not surprising, as the films in these foams are stabilized predominantly by surfactant molecules [16]. On the other hand, the yield stress of the CAPB + silica foams increased with time, due to particle aggregation, and the suspensions gradually gelled. As a result, the bubble Ostwald ripening gradually slowed down and eventually stopped completely [16].

Thus we see that different mechanisms are operative to suppress the bubble Ostwald ripening in these foams and those involving particle-assisted film and bubble stabilization are more efficient.

3.4. Viscosity of TTAB-silica suspensions and its effect on suspension foaminess

In our previous study of CAPB + silica system, we showed that the suspension foaminess depends primarily on the suspension viscosity under the conditions during foaming (e.g. same shear rate). In this section we check how relevant the CAPB-silica viscosity relation is to silica + TTAB suspensions. We measured the viscosity of silica + TTAB suspensions, using the procedure described in Section 2.4, which is designed to mimic the conditions during foaming as closely as possible.

The results for the time dependence of the viscosity for suspensions containing 15.7 wt% particles, at different surfactant concentrations (expressed as surface coverage, θ) are shown in Fig. 6. The silica suspensions with composition corresponding to Region 1UD behaved as Newtonian fluids - the viscosity of these suspensions did not depend on the shear rate and on the time of shearing (the two black curves in Fig. 6A). The viscosities of the suspensions without TTAB and at θ = 0.2% were both ≈4.5 mPa s. The viscosity

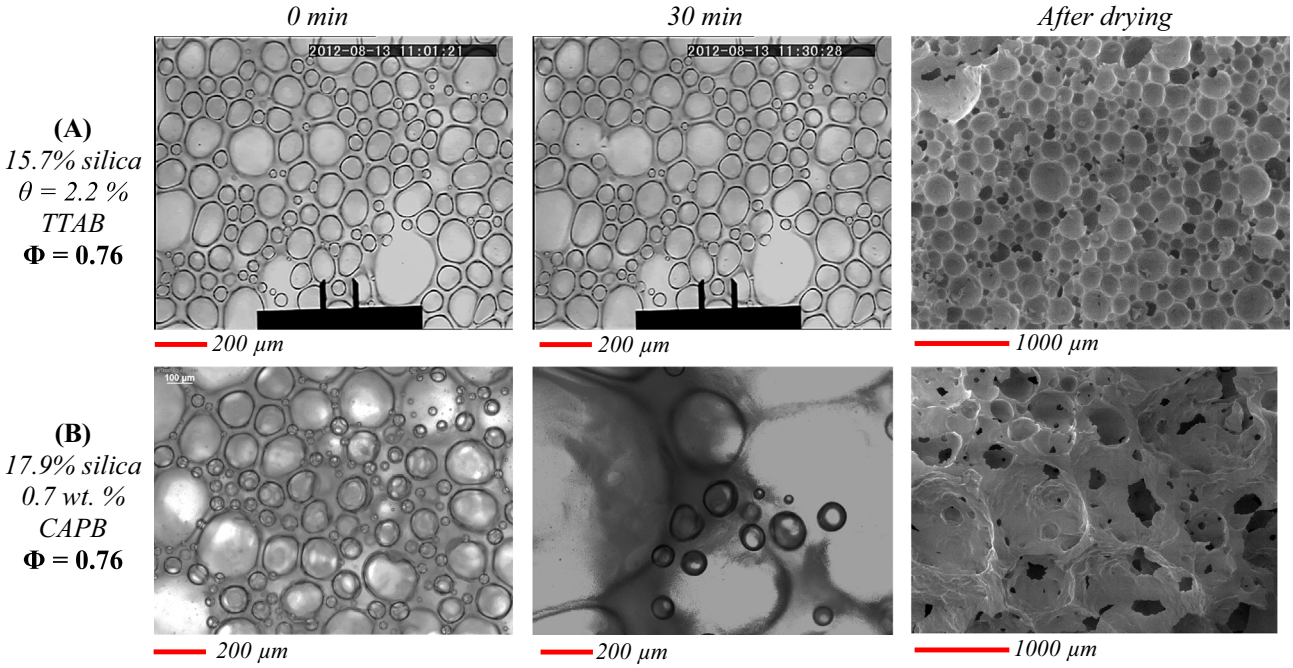

Fig. 5. Microscope images of bubbles in foams, immediately after their preparation and after 30 min, and SEM micrographs of the materials obtained after drying of these foams.

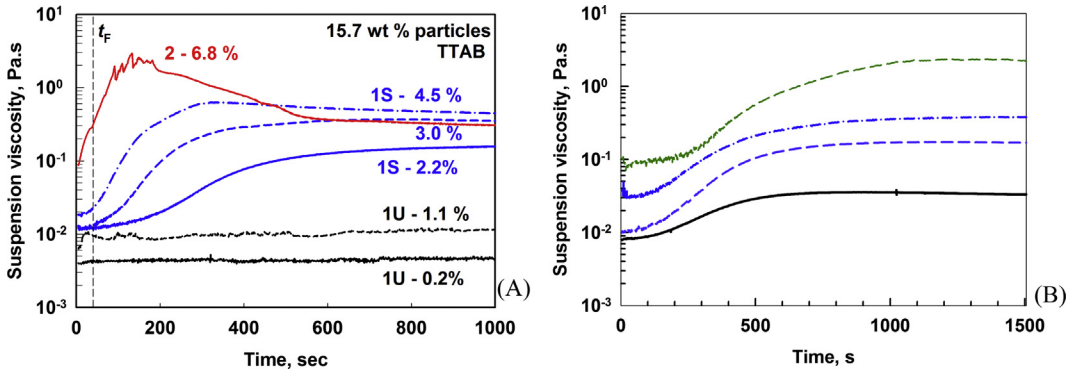

Fig. 6. Apparent viscosity as a function of time, for 15.7 wt% silica suspension (A) at shear rate of 100 s^{-1}, as a function of TTAB surface coverage of the particles, θ [%]. Color coding in the figure indicates the foaming regions, as in Fig. 2. (B) 15.7 wt% silica with 2.2% TTAB coverage, at different shear rates.

of the suspension with θ = 1.1% (corresponding to the boundary between Regions 1U and 1S) was ≈10 mPa s in the first 1000 s and slowly increased afterwards (data not shown). The foams prepared from the suspensions with this coverage had air volume fraction $\Phi_{PL} \approx 60 \pm 10$ vol%. However, these foams were unstable due to liquid drainage, related to the low yield stress of the suspension (see Section 3 in ESI) and the relatively large size of the bubbles, Fig. 4B.

The suspensions with composition in Region 1S showed more complex dependence η(*t*), see the blue curves in Fig. 6A. For all suspensions with θ between 2.2% and 4.5%, three well defined regions were observed: induction period in which η increased by less than 20%; fast increase of the viscosity by several times; and reaching an almost constant value.

The induction period was very important for the foam generation, because the suspension viscosity was still relatively low and the air entrapment was easy. Note that the foaming period in our experiments, during which the foam volume increases upon mixing, was usually shorter or comparable to the duration of the induction period in the respective curve η(*t*), see the dashed vertical line in Fig. 6A. After this induction period, the viscosity increased by >5 times for a short period of time and, afterwards, remained constant. The time for reaching this "plateau" viscosity was shorter at higher TTAB concentrations and upon faster mixing (see Fig. 6A and B).

The suspensions falling in Region 1UC by composition, where the foamability was low or negligible, had noticeably different dependence η(*t*), compared to those in Region 1S, see Fig. 6A. Induction period was not observed and the viscosity was much higher at the beginning of the rheological measurement/foaming, usually >100 mPa s. In most cases, we observed that the viscosity of these suspensions passed through a maximum and afterwards, decreased at longer times. The latter trend was considered as a sign of extensive particle aggregation and was found experimentally to be related to the formation of cracks in the respective drying foams.

Suspensions with composition corresponding to Region 2 (e.g., 13.5% TTAB coverage at C_p = 15.7 wt%) had shorter induction period than those in Region 1 – this period ended during the initial period of homogenization of the particle-surfactant mixture,

before foaming. The rheological properties of these samples could not be measured, because their apparent viscosity was well above 10 Pa s, immediately after loading these samples in the rheometer. This very high suspension viscosity led to difficult or even impossible air entrapment in the foaming stage.

From all these experiments we can conclude that the appropriate time-scale for foam formation from suspensions falling in region 1S coincides with the induction period, in which the suspension viscosity is still low and the air is easily trapped during stirring. In contrast, the subsequent plateau region in the curve $\eta(t)$ is associated with high suspension viscosity and, as a result, the used foaming device is unable to trap sufficient air volume. To check further this hypothesis we performed experiments in which TTAB was introduced in the suspension much earlier with respect to the start of the foaming stage. When we tried to trap air in this "aged" suspensions, containing 15.7 wt% particles and 6.8% TTAB coverage, we found that only ≈ 40 vol% air could be trapped after 10 min of mixing, whereas the suspension with the same composition gave foam with $\Phi_{PL} \approx 70\%$ in a regular experiment.

Therefore, to explain the suspension foaminess we should determine the suspension viscosity at the appropriate shear rate and aging time: Namely, at 30 ± 10 s for the higher shear rate (shown as dashed line in Fig. 6) and at 100 ± 25 s for the lower shear rate, after adding the surfactant into the silica suspension (see Fig. 1A and B). These aging times were used to extract data from the rheological curves $\eta(t)$ of the various suspensions.

In Fig. 7 we plot the air volume fraction in the plateau region, Φ_{PL}, as a function of the suspension viscosity, for the two shear rates used in the foaming experiments. One sees that all experimental data fall around a single (master) empirical curve, described by a power-law:

$$\Phi_{PL} \approx 0.34\eta^{-0.17} \quad (2)$$

where η is measured in mPa s and Φ_{PL} is dimensionless (varying between 0 and 1).

We compared the results obtained in this work to those obtained in Ref. [16] with silica + CAPB suspensions. The trend observed for Pickering foams, formed with TTAB, was qualitatively similar (lower foaminess at higher viscosity) but quantitatively rather different. The suspension foaminess was much lower, compared to CAPB + silica suspensions, in which the foam films were stabilized by surfactant molecules, not by particles. Therefore, the mechanism of foam stabilization (by surfactant or by particles) plays a significant role on the foaminess – less foam is produced, at the same suspension viscosity and otherwise similar conditions, with particle-stabilized bubbles.

To confirm the latter conclusion, we performed additional experiments in a large excess of free (unabsorbed) TTAB. For this purpose 5 wt% of TTAB was added to the silica suspension. The foaminess of this TTAB-containing suspension was boosted very significantly by the free surfactant present, which hydrophilized the silica particles and displaced them from the bubble surfaces. Furthermore, the foaminess in excess of TTAB was very close to the one of the CAPB-containing suspension with the same viscosity. Thus we have confirmed that the main difference between the two curves, shown in Fig. 7 for particle-stabilized and surfactant-stabilized foams, does not originate in the specific chemistry of the used surfactants but in the different mechanisms of foam stabilization.

A possible explanation of the reduced foaminess in the absence of free surfactant is that we increase the surface friction and, thus, we suppress very significantly the surface deformability when particles are adsorbed on the air-water interface [28,29]. Experimental confirmation of the reduced foamability in a planetary mixer upon increasing the surface viscoelasticity of the surfactant solutions was reported in Ref. [30]. Another possible explanation is that the particles are less efficient to stabilize the bubbles and they coalesce during foaming, due to the slower particle adsorption (as compared to surfactants) in the sheared foams [26]. Probably, both effects play a role in the observed lower foaminess of particle-stabilized foams.

3.5. Mechanical strength of the porous materials

To check whether the Pickering stabilization of foams provides higher mechanical strength of the final porous materials, we prepared wet foams with different bubble volume fractions. Upon drying, these foams produce porous materials with mass density proportional to the suspension fraction in the precursor wet foam, as predicted by our model [21]: $\rho = 474(1 - \Phi)$, where ρ is the mass density of the porous material [kg/m^3], 474 kg/m^3 is the mass density of the closed-packed particles in a dried suspension and Φ is the bubble volume fraction in the wet foam. More detailed information about the relations between the properties of the wet foam pre-cursor and the properties of the dry foam materials are presented in Ref. [21] along with the respective mechanistic explanations and theoretical model.

We measured the mechanical strength of the dried (non-sintered) porous materials using the procedure in Section 2.5 (see Section S2 in ESI for more details). These results are shown

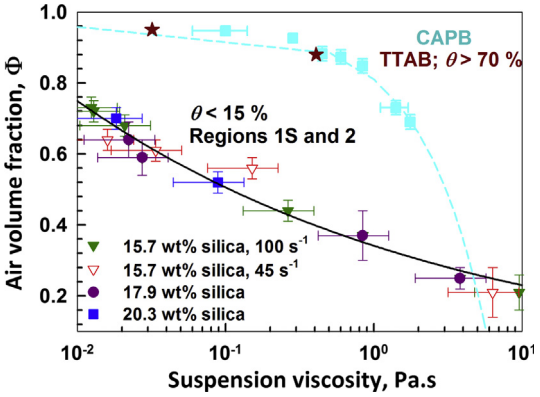

Fig. 7. Master curves and comparison of the air volume fraction Φ_{PL}, as a function of the viscosity of the suspension, used for foam formation. Lower (black) curve illustrates the results for Pickering-stabilized foams (TTAB), while the dashed line represents the case of mixed surfactant + particles stabilization (CAPB and large excess of TTAB).

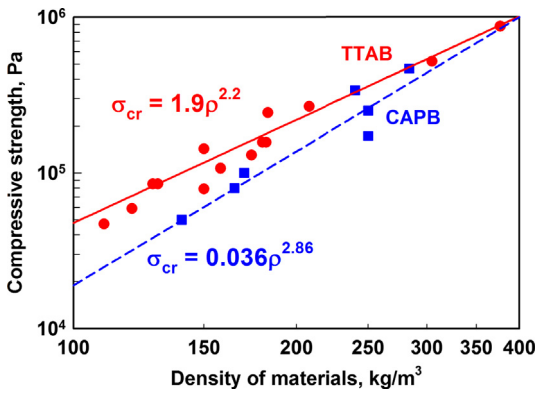

Fig. 8. Mechanical strength of the porous ceramic materials, as a function of their mass density. Red circles represent the Pickering foams, produced with TTAB, while the blue squares correspond to foams produced with CAPB, using the procedure from Ref. [16].

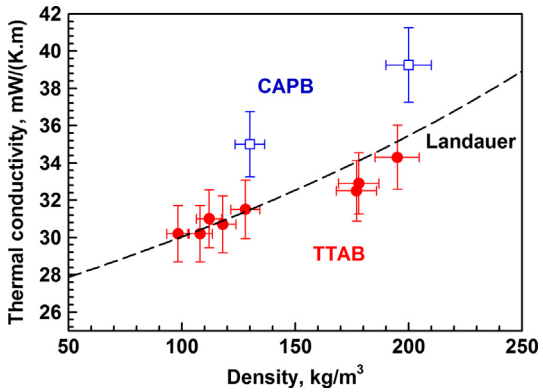

Fig. 9. Thermal conductivity of porous materials, as a function of their mass density. Red circles represent materials prepared via Pickering stabilization, while blue rectangles correspond to foams produced with CAPB, using the procedure from Ref. [16]. Landauer dependence (dashed curve) is calculated using 1400 mW/(K m) as a thermal conductivity of the bulk silica, 26 mW/(K m) for air and using Eq. (11) from Ref. [31].

in Fig. 8, as a function of the mass density of the dry porous materials. As expected, the mechanical strength of the materials followed power-law dependence and decreased with increasing of porosity. The strength of the materials, prepared in presence of TTAB was slightly higher than that of CAPB foams of the same mass density. However, considering the margin of the experimental error, this effect was non-negligible only at bubble volume fractions higher than close-packing, *ca.* $\Phi \geq 0.70$ (viz. at $\rho < 150$ kg/m^3), where the CAPB foams were less stable during drying, due to the high rates of bubble Ostwald ripening in the wet foam pre-cursor, e.g. Fig. 5B. Thus we see that an important advantage of the Pickering foams is that they are much more stable in the range of very high porosity, when the mass density of the final dry materials becomes below ca. 200 kg/m^3.

3.6. Thermal conductivity of the porous materials

Finally, we measured the thermal conductivity of the dry porous materials using the procedure from Section 2.6. Fig. 9 shows the thermal conductivity, as a function of the mass density of the materials. In general, the thermal conductivity decreased with the increase of air content in the porous materials. The materials obtained from TTAB-containing suspensions followed a Landauer dependence [31], taking 1400 mW/(K m) as bulk conductivity of the silica, Eq. (9) in Ref. [32].

The materials obtained from CAPB-containing suspensions had a higher conductivity by 3–5 mW/(K m) on average, when compared to TTAB samples. Since the CAPB foams did not contain large cracks at the densities studied, 130 kg/m^3 or higher, the higher thermal conductivity was attributed to the larger pores inside the CAPB foams (due to the extensive bubble Ostwald ripening). Indeed, it is known that the radiative component of the thermal conductivity is directly proportional to the pore size [33]. Thus we conclude that the Pickering foams have the important advantage of providing much smaller pores, even at a very high porosity of 90–95% voids in the dry material, due to the suppression of the bubble Ostwald ripening in the respective wet foam precursors.

4. Conclusions

In previous studies [6–9,16] several research groups showed that dry porous materials could be produced by foaming of suspensions, containing colloid particles and appropriate surfactants, followed by drying of the produced foams. Various combinations of particles and surfactants were successfully tested and explanations about the role of surfactant head-group were reported [7,8]. It was shown [16,34] that various processes could reduce the stability of the wet foam precursors, thus hampering the formation of stable porous materials. Still, the link between the main properties of the foamed suspensions, on one side, and the properties of the formed foams and porous materials, on the other side, has remained elusive, due to the complexity of the systems and processes involved.

In this study we compare the process of wet foam formation, the stability of the produced foams and some of the main properties of the final porous materials for concentrated silica suspensions, containing either the cationic surfactant TTAB or the zwitterionic surfactant CAPB. These two surfactants lead to very different foam types, particle-stabilized and surfactant-stabilized respectively, with a significant impact on the properties of the produced foams and of the final materials. Thus we could distinguish clearly between the general (common) features shared between various surfactant systems and those which are specific for a given surfactant.

The most important general (common) trends for both types of systems are:

(1) The suspension foaminess is controlled exclusively by the suspension viscosity under the shearing conditions which mimic closely the actual foaming process, viz. measured at the relevant (i) shear rate and (ii) aging time after mixing the surfactant and particles;
(2) The foam stability to drainage and coarsening is controlled exclusively by the suspension yield stress. Both the suspension viscosity and yield stress are governed by the particle-particle interactions in the suspensions which, in their turn, are affected by the surfactant adsorption on the particle surface;
(3) There are major kinetic effects of surfactant adsorption on the particle surface, within a time scale of seconds and minutes, which result in respective changes of the suspension rheological properties. Understanding and controlling these kinetic effects is crucial to ensure the required foaminess and foam stability in each particular system;
(4) There are general relations between the bubble size and mass density of the wet foam pre-cursor and the respective pore size and mass density of the dry foam materials, as explained in [21].

The most important surfactant-specific differences are the following:

(5) The foaminess of the suspensions leading to Pickering stabilization is much lower at the same suspension viscosity, as compared to suspensions leading to surfactant-stabilized foams. This difference emphasizes the important role of surface viscoelasticity – the much higher surface viscoelasticity, created by the particle adsorption layers [35,36], enhances the foam stability but reduces strongly the foaminess of the respective suspensions.
(6) Bubble Ostwald ripening in the wet foams is arrested completely by the particle (Pickering) stabilization only. The mechanism of bulk suspension gelation with CAPB showed significant bubble Ostwald ripening in the first few minutes after foaming, with a negative effect on the bubble size and on the stability of the drying foams. The attempt to block the Ostwald ripening in gelling systems results in low foaminess of the suspension.

(7) The stability of particle-stabilized (Pickering) foams is much better which allowed us to obtain dry porous materials with lower mass density, higher mechanical strength and lower thermal conductivity (despite the lower foaminess of these suspensions). These beneficial properties are related to the closed cell structure and the more homogeneous pore size distribution inside the materials.

All these conclusions may serve as a solid basis for the design of future experimental and theoretical studies in this area. For example, the kinetics of the particle hydrophobization and the related suspension rheological properties can be finely controlled by appropriate selection of the surfactant concentration and chain-length, including the use of mixtures with different chain-lengths. Furthermore, the observed kinetic effects of surfactant adsorption on particle surface could be of high interest to other colloid systems and processes, such as the kinetic control of particle-particle interactions in suspensions, the possibilities for kinetic control of the internal structure and properties of aerogels produced from such suspensions, control of the transient non-Newtonian flow of particulate gels, etc.

Acknowledgement

The authors are grateful to Dr. Mathieu Joanicot from Saint Gobain Research, Paris for the numerous useful discussions. The support of this study by Saint Gobain Research is gratefully acknowledged. The authors gratefully acknowledge the support from the Horizon 2020 project ID: 692146-H2020-eu.4.b "Materials Networking". The study is under the umbrella of the COST action MP1305 "Flowing matter".

Appendix A. Supplementary material

Supplementary data associated with this article can be found, in the online version, at http://dx.doi.org/10.1016/j.jcis.2017.05.036.

References

[1] J. Binner, Ceramic foams, in: M. Scheffler, P. Colombo (Eds.), Cellular Ceramics: Structure, Manufacturing, Properties and Applications, WILEY-VCH Verlag GmbH & Co. KGaA, Weinheim, 2005, pp. 33–56.
[2] A. Young, O. Ornatete, M. Janney, P. Menchhofer, Gelcasting of alumina, J. Am. Cer. Soc. 18 (1991) 612–618, http://dx.doi.org/10.1111/j.1151-2916.1991.tb04068.x.
[3] P. Sepulveda, J.G. Binner, Processing of cellular ceramics by foaming and in situ polymerisation of organic monomers, J. Eur. Ceram. Soc. 19 (1999) 2059–2066, http://dx.doi.org/10.1016/S0955-2219(99)00024-2.
[4] S. Dhara, P. Bhargava, Influence of slurry characteristics on porosity and mechanical properties of alumina foams, Int. J. Appl. Ceram. Technol. 3 (2006) 382–392, http://dx.doi.org/10.1111/j.1744-7402.2006.02098.x.
[5] E. Dickinson, R. Ettelaie, T. Kostakis, B.S. Murray, Factors controlling the formation and stability of air bubbles stabilized by partially hydrophobic silica nanoparticles, Langmuir 20 (2004) 8517–8525, http://dx.doi.org/10.1021/la048913k.
[6] B.P. Binks, T.S. Horozov, Aqueous foams stabilized solely by silica nanoparticles, Angew. Chemie Int. Ed. 44 (2005) 3722–3725, http://dx.doi.org/10.1002/anie.200462470.
[7] U.T. Gonzenbach, A.R. Studart, E. Tervoort, L.J. Gauckler, Ultrastable particle-stabilized foams, Angew. Chemie Int. Ed. 45 (2006) 3526–3530, http://dx.doi.org/10.1002/anie.200503676.
[8] U.T. Gonzenbach, A.R. Studart, E. Tervoort, L.J. Gauckler, Stabilization of foams with inorganic colloidal particles, Langmuir 22 (2006) 10983–10988, http://dx.doi.org/10.1021/la061825a.
[9] U.T. Gonzenbach, A.R. Studart, E. Tervoort, L.J. Gauckler, Tailoring the microstructure of particle-stabilized wet foams, Langmuir 23 (2007) 1025–1032, http://dx.doi.org/10.1021/la0624844.
[10] R. Deleurence, C. Parneix, C. Monteux, Mixtures of latex particles and the surfactant of opposite charge used as interface stabilizers – influence of particle contact angle, zeta potential, flocculation and shear energy, Soft Matter. 10 (2014) 7088–7095, http://dx.doi.org/10.1039/C4SM00237G.
[11] Z.-G. Cui, Y.-Z. Cui, C.-F. Cui, Z. Chen, B.P. Binks, Aqueous foams stabilized by in situ surface activation of $CaCO_3$ nanoparticles via adsorption of anionic surfactant, Langmuir 26 (2010) 12567–12574, http://dx.doi.org/10.1021/la1016559.
[12] Q. Liu, S. Zhang, D. Sun, J. Xu, Foams stabilized by Laponite nanoparticles and alkylammonium bromides with different alkyl chain lengths, Colloids Surfaces A Physicochem. Eng. Asp. 355 (2010) 151–157, http://dx.doi.org/10.1016/j.colsurfa.2009.12.003.
[13] C. Chuanuwatanakul, C. Tallon, D.E. Dunstan, G.V. Franks, Controlling the microstructure of ceramic particle stabilized foams: influence of contact angle and particle aggregation, Soft Matter. 7 (2011) 11464, http://dx.doi.org/10.1039/c1sm06477k.
[14] L.R. Arriaga, W. Drenckhan, A. Salonen, J.A. Rodrigues, R. Íñiguez-Palomares, E. Rio, D. Langevin, On the long-term stability of foams stabilised by mixtures of nano-particles and oppositely charged short chain surfactants, Soft Matter. 8 (2012) 11085, http://dx.doi.org/10.1039/c2sm26461g.
[15] A. Maestro, E. Rio, W. Drenckhan, D. Langevin, A. Salonen, Foams stabilised by mixtures of nanoparticles and oppositely charged surfactants: relationship between bubble shrinkage and foam coarsening, Soft Matter. 10 (2014) 6975–6983, http://dx.doi.org/10.1039/C4SM00047A.
[16] I. Lesov, S. Tcholakova, N. Denkov, Factors controlling the formation and stability of foams used as precursors of porous materials, J. Colloid Interface Sci. 426 (2014) 9–21, http://dx.doi.org/10.1016/j.jcis.2014.03.067.
[17] L.J. Gibson, M.F. Ashby, Cellular Solids: Structure and Properties, 2nd ed., Cambridge University Press, Cambridge, 1997.
[18] C. Totland, A.M. Blokhus, W. Nerdal, The nature of alcohol co-adsorption sites and their effects on surfactant aggregate structure on silica investigated by 2H and 13C NMR, RSC Adv. 3 (2013) 19117, http://dx.doi.org/10.1039/c3ra42495b.
[19] A.K.S. Chesterton, G.D. Moggridge, P.A. Sadd, D.I. Wilson, Modelling of shear rate distribution in two planetary mixtures for studying development of cake batter structure, J. Food Eng. 105 (2011) 343–350, http://dx.doi.org/10.1016/j.jfoodeng.2011.02.044.
[20] P. Petit, I. Javierre, P.-H.H. Jézéquel, A.-L.L. Biance, Generation and stability of bubbles in a cement based slurry, Cem. Concr. Res. 60 (2014) 37–44, http://dx.doi.org/10.1016/j.cemconres.2014.02.008.
[21] I. Lesov, S. Tcholakova, N. Denkov, Drying of particle-loaded foams for production of porous materials: mechanism and theoretical modeling, RSC Adv. 4 (2014) 811–823, http://dx.doi.org/10.1039/c3ra44500c.
[22] A. Scheludko, Thin liquid films, Adv. Colloid Interface Sci. 1 (1967) 391.
[23] V. Chaplain, P. Mills, G. Guiffant, P. Cerasi, Model for the flow of a yield fluid through a porous medium, J. Phys. II (2) (1992) 2145–2158, http://dx.doi.org/10.1051/jp2:1992257.
[24] S. Tcholakova, Z. Mitrinova, K. Golemanov, N.D. Denkov, M. Vethamuthu, K.P. Ananthapadmanabhan, Control of Ostwald ripening by using surfactants with high surface modulus, Langmuir 27 (2011) 14807–14819, http://dx.doi.org/10.1021/la203952p.
[25] M. Abkarian, A.B. Subramaniam, S.-H. Kim, R.J. Larsen, S.-M. Yang, H.A. Stone, Dissolution arrest and stability of particle-covered bubbles, Phys. Rev. Lett. 99 (2007) 188301, http://dx.doi.org/10.1103/PhysRevLett. 99.188301.
[26] S. Tcholakova, N.D. Denkov, A. Lips, Comparison of solid particles, globular proteins and surfactants as emulsifiers, Phys. Chem. Chem. Phys. 10 (2008) 1608, http://dx.doi.org/10.1039/b715933c.
[27] A. Cervantes Martinez, E. Rio, G. Delon, A. Saint-Jalmes, D. Langevin, B.P. Binks, On the origin of the remarkable stability of aqueous foams stabilised by nanoparticles: link with microscopic surface properties, Soft Matter. 4 (2008) 1531, http://dx.doi.org/10.1039/b804177f.
[28] C. Planchette, A.-L. Biance, O. Pitois, E. Lorenceau, Coalescence of armored interface under impact, Phys. Fluids 25 (2013) 42104, http://dx.doi.org/10.1063/1.4801320.
[29] D.Y. Zang, E. Rio, G. Delon, D. Langevin, B. Wei, B.P. Binks, Influence of the contact angle of silica nanoparticles at the air–water interface on the mechanical properties of the layers composed of these particles, Mol. Phys. 109 (2011) 1057–1066, http://dx.doi.org/10.1080/00268976.2010.542778.
[30] N. Politova, M.Sc. thesis "Factors Affecting the Processes During foam Formation" (in Bulgarian), 2012, Sofia University, Library address: <http://www.lib.chem.uni-sofia.bg>.
[31] D.S. Smith, A. Alzina, J. Bourret, B. Nait-Ali, F. Pennec, N. Tessier-Doyen, K. Otsu, H. Matsubara, P. Elser, U.T. Gonzenbach, Thermal conductivity of porous materials, J. Mater. Res. 28 (2013) 2260–2272, http://dx.doi.org/10.1557/jmr.2013.179.
[32] T. Xie, Y.-L. He, Z.-J. Hu, Theoretical study on thermal conductivities of silica aerogel composite insulating material, Int. J. Heat Mass Transf. 58 (2013) 540–552, http://dx.doi.org/10.1016/j.ijheatmasstransfer.2012.11.016.
[33] B.P. Jelle, A. Gustavsen, R. Baetens, The path to the high performance thermal building insulation materials and solutions of tomorrow, J. Build. Phys. 34 (2010) 99–123, http://dx.doi.org/10.1177/1744259110372782.
[34] A.R. Studart, U.T. Gonzenbach, E. Tervoort, L.J. Gauckler, Processing routes to macroporous ceramics: a review, J. Am. Ceram. Soc. 89 (2006) 1771–1789, http://dx.doi.org/10.1111/j.1551-2916.2006.01044.x.
[35] M. Safouane, D. Langevin, B.P. Binks, Effect of particle hydrophobicity on the properties of silica particle layers at the air-water interface, Langmuir 23 (2007) 11546–11553, http://dx.doi.org/10.1021/la700800a.
[36] C. Planchette, E. Lorenceau, A.-L. Biance, Surface wave on a particle raft, Soft Matter 8 (2012) 2444–2451, http://dx.doi.org/10.1039/C2SM06859A.